

Cryogenic Eyesafer Laser Optimization for Use Without Liquid Nitrogen

by Larry D. Merkle and Nikolay Ter-Gabrielyan

ARL-TR-6826

February 2014

NOTICES

Disclaimers

The findings in this report are not to be construed as an official Department of the Army position unless so designated by other authorized documents.

Citation of manufacturer's or trade names does not constitute an official endorsement or approval of the use thereof.

Destroy this report when it is no longer needed. Do not return it to the originator.

Army Research Laboratory

Adelphi, MD 20783-1197

ARL-TR-6826**February 2014**

Cryogenic Eyesafer Laser Optimization for Use Without Liquid Nitrogen

Larry D. Merkle and Nikolay Ter-Gabrielyan
Sensors and Electron Devices Directorate, ARL

Approved for public release; distribution unlimited.

REPORT DOCUMENTATION PAGE				Form Approved OMB No. 0704-0188	
<p>Public reporting burden for this collection of information is estimated to average 1 hour per response, including the time for reviewing instructions, searching existing data sources, gathering and maintaining the data needed, and completing and reviewing the collection information. Send comments regarding this burden estimate or any other aspect of this collection of information, including suggestions for reducing the burden, to Department of Defense, Washington Headquarters Services, Directorate for Information Operations and Reports (0704-0188), 1215 Jefferson Davis Highway, Suite 1204, Arlington, VA 22202-4302. Respondents should be aware that notwithstanding any other provision of law, no person shall be subject to any penalty for failing to comply with a collection of information if it does not display a currently valid OMB control number.</p> <p>PLEASE DO NOT RETURN YOUR FORM TO THE ABOVE ADDRESS.</p>					
1. REPORT DATE (DD-MM-YYYY) February 2014		2. REPORT TYPE Final		3. DATES COVERED (From - To)	
4. TITLE AND SUBTITLE Cryogenic Eyesafer Laser Optimization for Use Without Liquid Nitrogen				5a. CONTRACT NUMBER	
				5b. GRANT NUMBER	
				5c. PROGRAM ELEMENT NUMBER	
6. AUTHOR(S) Larry D. Merkle and Nikolay Ter-Gabrielyan				5d. PROJECT NUMBER	
				5e. TASK NUMBER	
				5f. WORK UNIT NUMBER	
7. PERFORMING ORGANIZATION NAME(S) AND ADDRESS(ES) U.S. Army Research Laboratory ATTN: RDRL-SEE-M 2800 Powder Mill Road Adelphi, MD 20783-1197				8. PERFORMING ORGANIZATION REPORT NUMBER ARL-TR-6826	
9. SPONSORING/MONITORING AGENCY NAME(S) AND ADDRESS(ES)				10. SPONSOR/MONITOR'S ACRONYM(S)	
				11. SPONSOR/MONITOR'S REPORT NUMBER(S)	
12. DISTRIBUTION/AVAILABILITY STATEMENT Approved for public release; distribution unlimited.					
13. SUPPLEMENTARY NOTES					
14. ABSTRACT <p>We report our efforts and findings on a High Energy Lasers Joint Technology Office (HEL-JTO)-funded project to identify and optimize Er-doped laser materials and lasing schemes for cryogenic operation without the need for liquid cryogenics. This calls for optimal performance around 125–150 K—high enough for reasonably efficient operation of a Stirling cooler. We investigated Er-doped yttrium aluminum garnet (Er:YAG) and Er-doped sesquioxides. We observe that the most favorable pump line in Er:YAG, at 1532 nm, is extremely narrow at 77 K, but that by 120–150 K it is broad enough for pumping by line-narrowed diodes. That material's laser output under narrow-band diode pumping is most efficient around 120 K and its laser wavelength is 1618 nm. Among the sesquioxides, Er:Sc₂O₃ looks most promising. It has strong emission lines at shorter wavelengths, yet long enough that at cryogenic temperatures their absorption is weak. The 1535 nm pump line of Er:Sc₂O₃ is sufficiently wide for efficient pumping by line-narrowed diodes. We observe efficient laser operation at 1581 nm and 1558 nm. Surprisingly, the latter line outperforms the former as the temperature is increased above liquid nitrogen temperature. Spectroscopic studies have clarified the reason for this encouraging small-quantum defect behavior.</p>					
15. SUBJECT TERMS Erbium, cryogenic, laser, YAG Sc203, sesquioxide					
16. SECURITY CLASSIFICATION OF:			17. LIMITATION OF ABSTRACT UU	18. NUMBER OF PAGES 24	19a. NAME OF RESPONSIBLE PERSON Larry D. Merkle
a. REPORT Unclassified	b. ABSTRACT Unclassified	c. THIS PAGE Unclassified			19b. TELEPHONE NUMBER (Include area code) (301) 394-0942

Contents

List of Figures	iv
List of Tables	iv
1. Motivation for This Study	1
2. Er:YAG	3
3. Er:Sc₂O₃	8
4. Potential Excited State Absorption in Er:YAG and Er:Sc₂O₃	12
5. Summary and Conclusions	14
6. References	17

List of Figures

Figure 1.)a)Temperature dependence of 2% Er:YAG laser output for constant incident pump pulse energy. The pump diode array had a central wavelength of 1530 nm and 9 nm full width at half maximum (FWHM). (b) Energy level diagram, showing the initial and final energy levels for the pump and laser transitions.....	2
Figure 2. Er:YAG absorption and stimulated emission cross section spectra at 77 K.	4
Figure 3. Temperature dependence of Er:YAG laser output for constant incident pump power, using pump diodes with 0.3-nm FWHM.	5
Figure 4. Product of absorption and laser initial state thermal populations versus temperature for Er:YAG lasers pumped at 1532 nm and lasing at either 1618 or 1645 nm.....	6
Figure 5. Expanded portion of the 77-K Er:YAG absorption and stimulated emission cross section spectra.	7
Figure 6. (a) Stimulated emission spectra of Er:YAG at intermediate temperatures. (b): Energy levels and related pump and laser transitions.	8
Figure 7. Absorption and stimulated emission cross section spectra of Er:Sc ₂ O ₃ at 77 K, in the spectral region near 1.5 microns.	9
Figure 8. Er:Sc ₂ O ₃ laser performance at 77 K, pumping at 1535 nm and with cavity optics chosen to select for lasing at 1558 nm.	10
Figure 9. (a) Absorption (dashed curves) and stimulated emission (solid curves) of Er:Sc ₂ O ₃ at three temperatures (red: 77 K; green: 100 K; blue: 150 K); (b) Energy levels of Er:Sc ₂ O ₃ , indicating the three overlapping transitions at 1558 nm.	11
Figure 10. Absorption spectrum of Er:Sc ₂ O ₃ zero-line region at two temperatures.....	12

List of Tables

Table 1. Measured width of the 1532-nm absorption line in Er:YAG at several temperatures. Data taken at and below 150 K were taken using a line-narrowed diode laser. Data at the higher temperatures were taken by spectrophotometer.....	4
Table 2. Potential for excited state absorption at existing or candidate laser wavelengths in the materials under study.	14

1. Motivation for This Study

Given the importance of high beam quality, high efficiency, and excellent thermal management for high power solid-state lasers, there is much to commend cryogenic operation. In most crystalline and high quality polycrystalline materials, thermal conductivity becomes considerably larger as the temperature is reduced from 300 K to around 100 K, whereas the coefficient of thermal expansion and the thermo-optic coefficient decrease. Together, these greatly reduce the thermally induced beam distortion caused by a given thermal load. However, the most straightforward means of maintaining the laser at cryogenic temperatures is by contact with liquid nitrogen. This adds a complication to the logistics of high power laser operation, particularly in applications that require mobility or transportability. If a solid-state laser system with an optimum operating temperature somewhat higher—ideally 125–150 K—can be identified, then a Stirling cooler can be used to maintain that temperature without cryogenic liquids. It was the purpose of this study to investigate the material properties and operating parameters needed to optimize laser performance in the desired temperature range. This did not include actual use of Stirling coolers, but rather involved both spectroscopic studies of material properties and laser testing, the latter to determine the factors not accessible by spectroscopy and to evaluate power scaling potential.

A related goal was to determine the quantum efficiency of the candidate laser materials' upper laser levels, a highly relevant factor since it affects the heat deposition for a given laser output. However, due to the duration of this project, the quantum efficiency measurement did not continue long enough to obtain results, and thus will not be reported here.

This project concentrated on Er-doped laser materials lasing at wavelengths around 1.6 microns. Such wavelengths are in the band for which the eye is least susceptible to laser-induced damage, an important consideration for the minimization of collateral damage. Wavelengths longer than the more common one-micron region also have propagation advantages in high-scattering conditions, while still being short enough that diffraction is a lesser restriction on beam collimation than is true for HF, DF, or CO₂ lasers.

Additional motivation for this project came from an observation made in our recent study of cryogenic laser operation of erbium-doped yttrium aluminum garnet (Er:YAG) under broadband diode pumping (*1*). As shown in figure 1, for fixed incident pump power, the maximum laser output occurred at about 160 K. Analysis showed that this was due in part to the broadband nature of the pumping, such that thermal broadening of the absorption lines improved pumping efficiency. By itself, this factor points to the value of line-narrowing diode lasers. However, the analysis also showed that the phenomenon was caused in part by thermal occupation of the upper

laser level, so that increased temperature increases the effective gain cross section until line broadening and thermal population of the lower laser level eventually overcome that advantage. This process favors temperatures somewhat above liquid nitrogen temperature in Er:YAG, regardless of pump linewidth, and raises the possibility that similar—or even more favorable—situations may arise in other Er-doped materials.

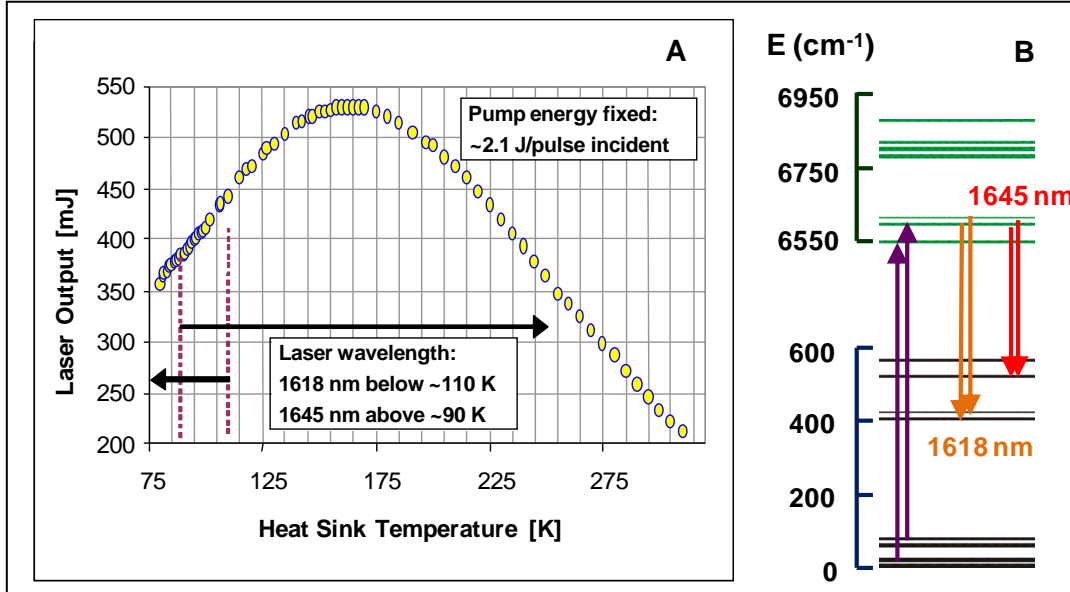


Figure 1. (a) Temperature dependence of 2% Er:YAG laser output for constant incident pump pulse energy. The pump diode array had a central wavelength of 1530 nm and 9 nm full width at half maximum (FWHM). (b) Energy level diagram, showing the initial and final energy levels for the pump and laser transitions.

A comment is in order regarding the importance of optimization in any effort to rely on Stirling (or other mechanical) coolers rather than liquid nitrogen. The target temperature range of this study, around 125–150 K, is near the point at which a Carnot cycle cooler would have a coefficient of performance of one—so that it would take a Watt of power for the cooler to “lift” each Watt of waste heat up to room temperature for removal. Commercial Stirling refrigerators have their optimal coefficient of performance for temperatures in that same region, but that optimal value is only 0.20 to 0.25, so that it would take 4–5 W to lift each Watt of waste heat. However, several factors can be optimized to reduce the heat load that must be extracted. These include selecting a pump wavelength and a laser wavelength that are very close (thus minimizing quantum defect), selecting a gain medium with maximum quantum efficiency, using low Er^{3+} concentration (to minimize upconversion), optimizing the overlap of pump beam and laser mode, and allowing as much as practicable of the medium’s fluorescence to exit the cryostat. If these can be optimized simultaneously, the amount of heat to be extracted by the Stirling cooler may be as little as 2–3% of the laser output power. (These estimates assume the use of the pump-lase schemes with the smallest quantum defects observed in this project, pumping at 1535 nm and

lasing at 1558 or 1581 nm in Er:Sc₂O₃.) Thus, the cooler's energy budget would be ~8–12% of the output power—quite reasonable in light of other portions of the energy budget, such as the 40–50% of total input power converted to heat in the pump diodes. (That is, the amount of power converted to heat in the pump diodes is very roughly equal to the laser's output power, even in a highly efficient laser.)

The study reported here concentrated on two classes of laser host material. The first was YAG, which has a combination of thermal, mechanical, and spectroscopic properties that has made it a singularly successful laser host since almost the beginning of the laser. The other class comprises the cubic sesquioxides, which have better thermal properties than YAG (2–4). Due in part to our initial assessment of the relative advantages of various Er-doped sesquioxides, and in part to the optical quality of available samples, we have concentrated most of our effort on one such sesquioxide, Sc₂O₃.

2. Er:YAG

The absorption and stimulated emission cross-section spectra of the Er:YAG $^4I_{15/2} \leftrightarrow ^4I_{13/2}$ transitions at a temperature of 77 K are shown in figure 2. In the interest of minimizing thermal load, it is desirable to diode-pump an Er:YAG laser at the longest-wavelength strong absorption peak, which is at 1532 nm. The stimulated emission transitions that lase most readily are those at 1618 and 1645 nm, for which 1532-nm pumping gives quantum defects of 5.6% and 7.4%, respectively, in contrast to the 10–12% quantum defect that one would obtain by pumping the peaks around 1470 nm.

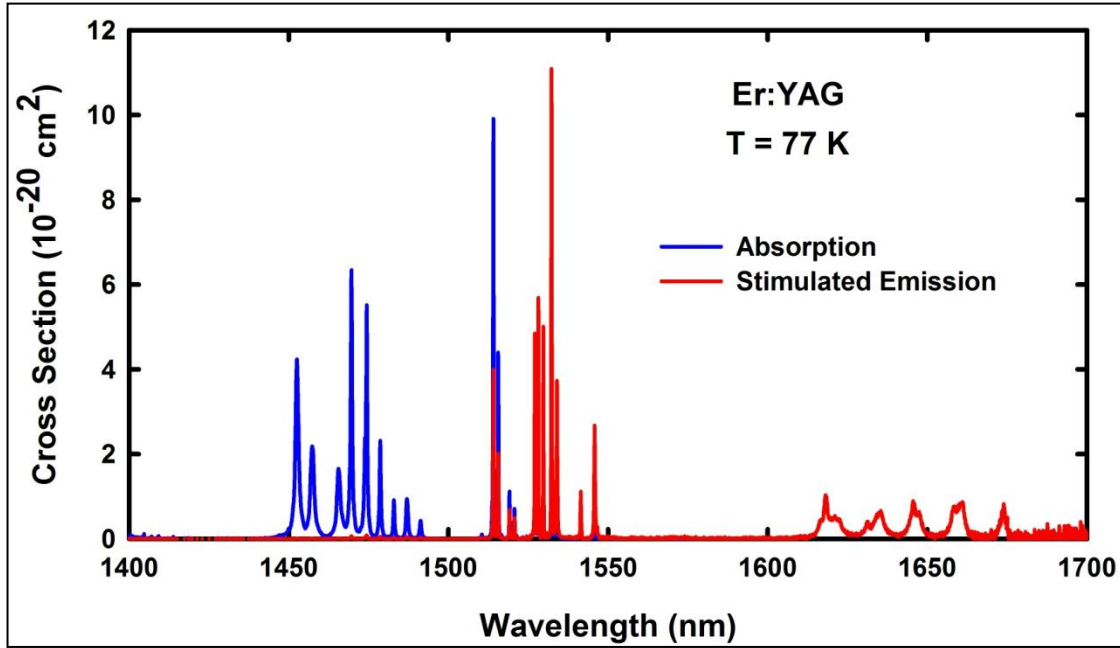


Figure 2. Er:YAG absorption and stimulated emission cross section spectra at 77 K.

However, use of this 1532-nm absorption line for diode pumping at cryogenic temperatures presents a challenge, due to the very narrow width of that line. We have measured that as a function of temperature, and have discovered that at very low temperatures it is too narrow for accurate use of our Cary absorption spectrophotometer. We had to use an external cavity, single-mode, tunable diode laser to scan across that line to determine its width. The results are given in table 1.

Table 1. Measured width of the 1532-nm absorption line in Er:YAG at several temperatures. Data taken at and below 150 K were taken using a line-narrowed diode laser. Data at the higher temperatures were taken by spectrophotometer.

T (K)	FWHM (nm)
77	0.023
100	0.037
125	0.082
150	0.119
225	0.42
300	0.68

The challenge involved here is that pumping by diode lasers with greater spectral width than these values will result in inefficient pump absorption. Spectral narrowing of diode lasers has made great progress, with the diodes accessible to us ranging from 9 nm FWHM when we first began working with diode pumping of Er:YAG at room temperature, to 0.2 nm FWHM in a

230 W diode matrix from CREOL (U. of Central Florida), made available to us in the present study. Despite so much progress, really efficient absorption of the pump light by the 1532-nm peak of Er:YAG would require temperatures above 150 K. No doubt further progress in line narrowing can be expected, facilitating pumping at somewhat lower temperatures, but the highly efficient use of this peak at temperatures near 77 K would require rather extreme narrowing.

Despite its narrow width, diode pumping of the 1532-nm peak can yield useful and reasonably efficient lasing. Employing a PLI (Princeton Lightwave) pump diode stack with 0.3-nm FWHM, we carried out a temperature-dependent lasing experiment under constant pump power similar to that of figure 1. The results are shown in figure 3. These data are obtained by the measurement of individual quasi-CW pulses after the output is separated using diffraction gratings. The detection system could measure the pulses of only one wavelength at a time, and we suspect that no single laser pulse emitted both wavelengths at once. Thus, the appearance of data points in figure 3 that seem to add up to far more than 2 W is just an artifact of the output monitoring. Due to the narrower pump linewidth, the effect of improved absorption with increasing temperature is somewhat less than in the broadband-pumped case of figure 1. As a result, the laser performance does not increase greatly with temperature, but it does remain quite strong up to at least 170 K. With wavelength selective optics to suppress 1645-nm oscillation, the 1618-nm output peaked at ~ 120 K and decreased by only 20% at 160 K. This drop-off with temperature is faster than for 1645-nm laser operation due to growth with temperature of the more significant absorption at 1618 nm.

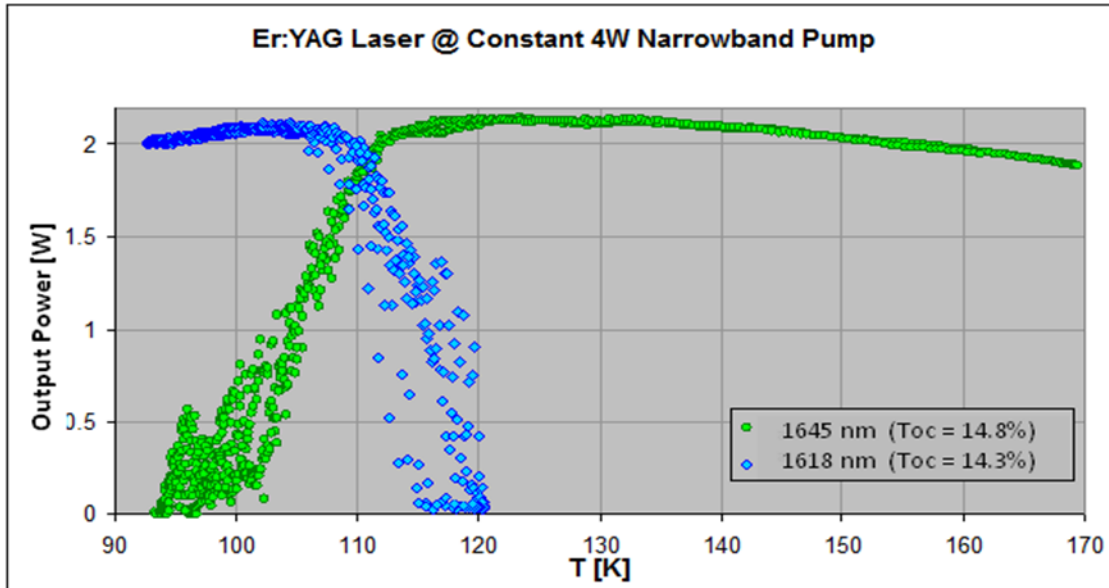


Figure 3. Temperature dependence of Er:YAG laser output for constant incident pump power, using pump diodes with 0.3-nm FWHM.

Since the improvement in pump efficiency due to thermal line broadening is probably weaker in this narrow-band pumping case than for broad-band pumping, the thermal population of the initial states of both the pump and laser transitions should have a more evident effect on the laser temperature dependence. The product of these population factors can be calculated simply. The 1532-nm pump transition's initial state is 22 cm^{-1} above the ground state, and the initial level for both the 1618-nm and 1645-nm laser transitions lies about 50 cm^{-1} above the bottom of the $^4I_{13/2}$ manifold. The full set of energy levels for each manifold can be used to calculate the partition functions for each desired temperature, resulting in the product of population factors shown in figure 4. With its peak at 125 K and slow drop-off at higher temperatures, this product resembles the 1645-nm laser output's temperature dependence quite closely.

It would be desirable to lase at a shorter wavelength, thus decreasing the quantum defect, if spectroscopic properties enable efficient operation. At 77 K, Er:YAG has no significant emission features at wavelengths between 1546 and 1616 nm. Figure 5 shows the 1520–1560-nm portion of the 77-K absorption and stimulated emission spectrum, in which we see that, of the peaks shorter than the 16xx region, only the peak at 1546 nm has stimulated emission sufficiently greater than absorption for laser operation to be a serious option. In this program we attempted to lase that line while pumping at 1532 nm, which would give a quantum defect of only 0.9%, but without success. The absorption is sufficiently large to yield an unreasonably high threshold.

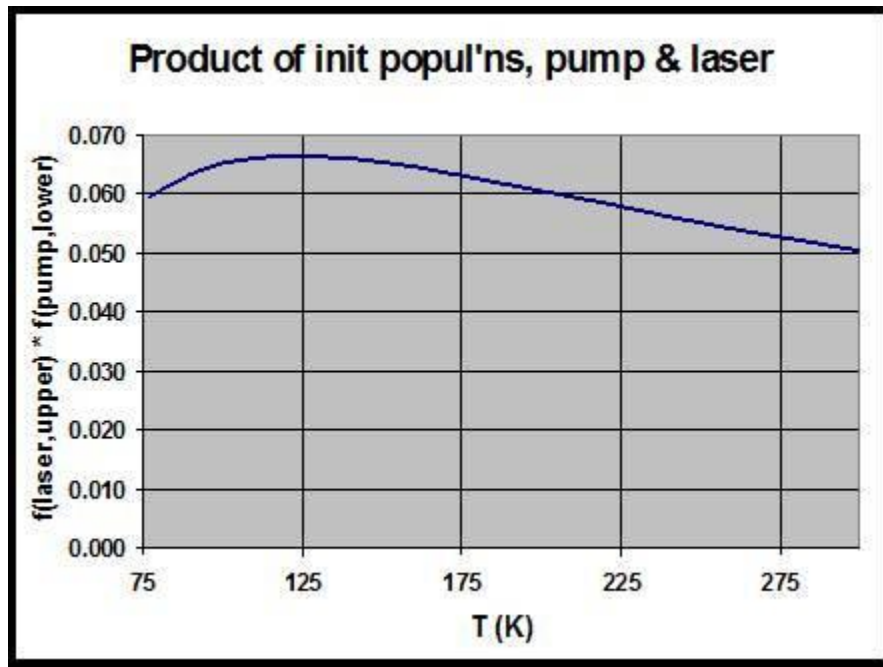


Figure 4. Product of absorption and laser initial state thermal populations versus temperature for Er:YAG lasers pumped at 1532 nm and lasing at either 1618 or 1645 nm.

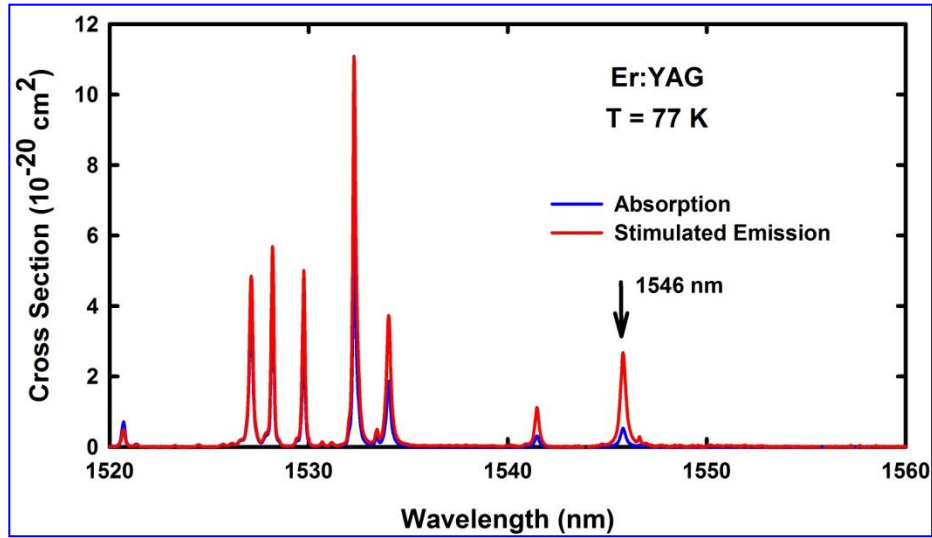


Figure 5. Expanded portion of the 77-K Er:YAG absorption and stimulated emission cross section spectra.

Since the absorption at 1546 nm is, indeed, substantial, we then tried *pumping* that line to drive lasing at 1618 nm. This provides only a modest reduction of quantum defect relative to 1532-nm pumping, from 5.6% to 4.7%, but it does work. Not surprisingly, the laser performance with respect to absorbed pump power is practically identical to that for 1532-nm pumping. This is a potentially practical pump-lase scheme, but due to the much smaller absorption at 1546 nm as compared to 1532 nm, careful design would be required to achieve efficient pump absorption.

At temperatures around 130 K, we did achieve lasing on a different short-wavelength line, namely 1565 nm. This emission is not even detectable in our 77-K fluorescence spectra, but becomes measurable by 100 K. The spectra of figure 6A indicate that the stimulated emission cross section of this line is considerably smaller than for the 1546-nm line, but lasing is more readily achievable at 1565 nm because its absorption not shown is much weaker. The neighboring peak at 1572 nm has somewhat larger stimulated emission and smaller absorption, but the wavelength selectivity of the mirror set, chosen to suppress 1618 and 1645 nm, favored 1565 nm. Figure 6B shows the Er:YAG $^4I_{13/2}$ and $^4I_{15/2}$ manifolds, and the various transitions discussed in this section. Note that there are two very close transitions at about 1565 nm, and it is not certain which one is lasing. The candidate upper laser levels lie about $200\text{--}225\text{ cm}^{-1}$ above the upper levels of the 1618 and 1645-nm transitions, so that even at 150 K the thermal population of the former is small compared to that of the latter. To appear in the spectra at as low a temperature as 100 K and to lase by 130 K, at least one of the transitions at 1565 nm must have very substantial line strength. However, due to the upper states' small thermal populations for any reasonable temperature, we do not propose these remarkable lines for practical laser operation.

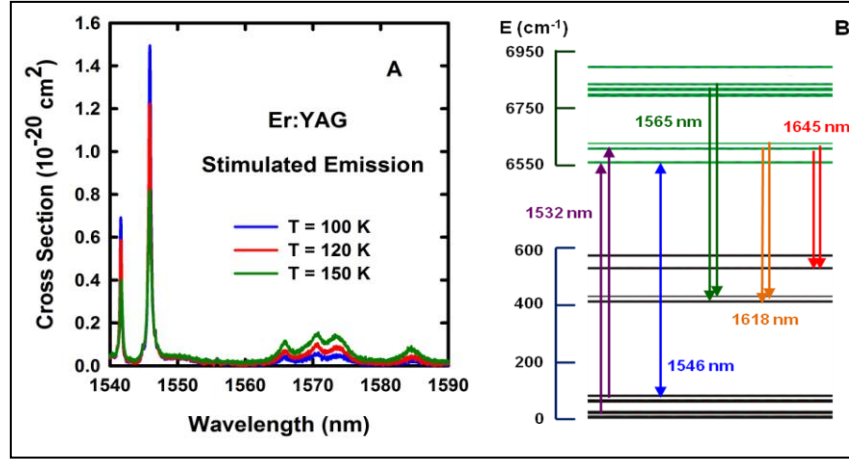


Figure 6. (a) Stimulated emission spectra of Er:YAG at intermediate temperatures. (b): Energy levels and related pump and laser transitions.

3. Er:Sc₂O₃

The geometry of the cation sites in sesquioxides (Sc^{3+} in Sc_2O_3 , Y^{3+} in Y_2O_3 , etc.) is sufficiently different from that of the Y^{3+} site in YAG that the pattern of Er^{3+} energy levels is quite different, including the $^4\text{I}_{15/2}$ ground manifold of particular relevance for lasing at wavelengths near 1.5–1.6 microns. The resulting differences in spectra can be quite important for laser operation. The absorption and stimulated emission cross-section spectra of Er:Sc₂O₃ $^4\text{I}_{13/2} \leftrightarrow ^4\text{I}_{15/2}$ transitions at 77 K are shown in figure 7. It should be noted that these cross sections were calculated assuming that the dopant ions enter this host's two different cation sites with equal probability, so that three-quarters reside in the sites with C_2 symmetry and one-quarter in the sites with C_{3i} symmetry.

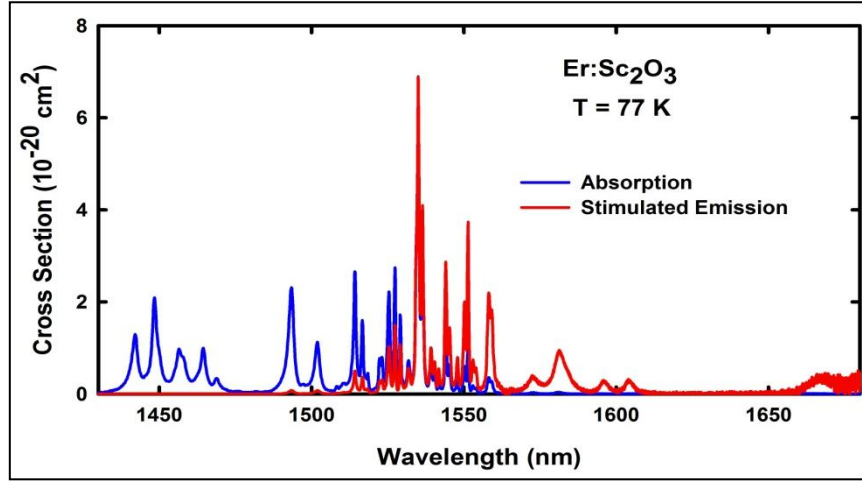


Figure 7. Absorption and stimulated emission cross section spectra of Er:Sc₂O₃ at 77 K, in the spectral region near 1.5 microns.

Comparison to the analogous Er:YAG spectra in figure 2 reveals a number of differences, at least two of which are important to our search for efficient laser operation with minimal heat loading at temperatures sufficiently above liquid nitrogen temperature to permit use of a Stirling cooler. The emission peaks beyond 1600 nm in Er:Sc₂O₃ have only about one-third the maximum cross section of the similarly situated peaks of Er:YAG. The situation is similar at room temperature so that at any temperature, if laser operation at those long wavelengths is desired, Er:YAG is likely to be a better choice than Er:Sc₂O₃ (or any Er-doped sesquioxide). However, in the region between ~1550 nm and ~1610 nm, where Er:YAG has no measurable spectral features at 77 K, Er:Sc₂O₃ has several emission peaks. In particular, the Er:Sc₂O₃ peak at 1581 nm is approximately as strong as the best of the longer-wavelength Er:YAG peaks, yet is still far enough from the “zero line” (the transition between the bottom-most levels of the two manifolds) to have insignificant absorption at 77 K. Lasing this transition, coupled with pumping of the strong absorption line at 1535 nm (the nearest analog to the Er:YAG 1532-nm line), gives a quantum defect of only 3.0%. An intriguing candidate for lasing is the line at approximately 1558 nm. Its stimulated emission cross section at 77 K is about the same as the Er:YAG 1546-nm peak, but its absorption is weaker. This difference is due to the 1558-nm peak’s slightly greater separation from the Er:Sc₂O₃ zero line than is true for the Er:YAG peak, and we have found that difference to be very important. Laser operation on this emission line with 1535-nm pumping gives a very small quantum defect of 1.5%.

In the course of this study, we found that both the 1581-nm and 1558-nm lines of Er:Sc₂O₃ do lase, and do so with reasonably good efficiency. (Due to the exploratory nature of the one funded year of this study, these and all the lasers reported here can almost surely be further optimized.) An example of the performance of the 1558-nm laser is given in figure 8. Absorbed pump power (P_{abs}) was derived from simultaneous measurements of the incident pump power

(P_{in}) and the total laser output (P), which consisted of the laser signal (P_L) and unabsorbed pump (P_{up}) leaked through the output coupler with T_{OC} transmission at the wavelength of pump, $P = P_L + P_{up}$. The two signals were separated by dispersing optics (gratings), and were recorded simultaneously and corrected for the grating efficiency using a LabView interface. The absorbed pump power is then simply $P_{abs} = P_{in} - P_{up}/T_{OC}$. This formula neglects the portion of pump that was unabsorbed on the first pass and reflected back into the laser mode volume by the output coupler. The impact of this portion was estimated at less than 5%.

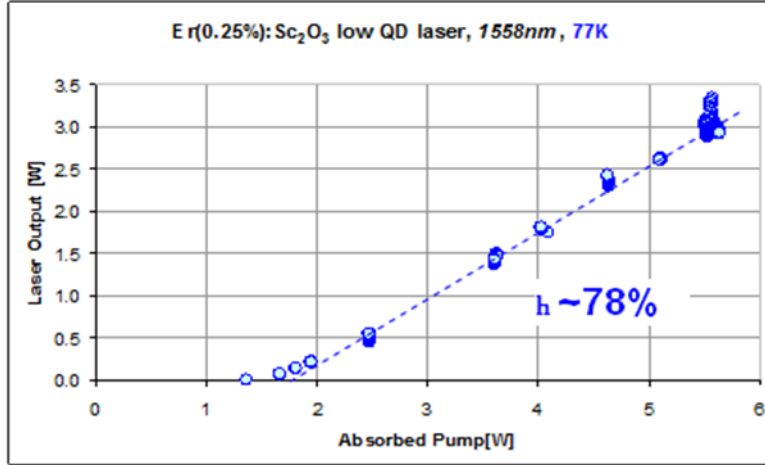


Figure 8. Er:Sc₂O₃ laser performance at 77 K, pumping at 1535 nm and with cavity optics chosen to select for lasing at 1558 nm.

We have found that, due to the significantly different absorption and gain of the 1558- and 1581-nm lines, we can select for one transition or the other by the choice of output coupler reflectivity, even if that reflectivity is spectrally flat. For output coupler reflectivity greater than approximately 0.95, the laser operates at 1581 nm, as the absorption at 1558 nm gives too much loss. For reflectivity less than 0.80, the laser operates at 1558 nm, because that line's absorption is now minor compared with the 20% outcoupling loss and that high loss requires the larger gain of the 1558-nm line. (For intermediate reflectivities, both lines can lase depending on pump power and, thus, presumably temperature.)

As of the conclusion of this project, we had observed that the efficiency of 1558-nm lasing remained reasonably constant up to at least 110 K. More recently, we have observed that it remains reasonably efficient up to 160 K. We have also subsequently observed that above 110 K, the laser switches to 1558-nm operation even for high output coupler reflectivity. The reason for this rests upon spectroscopy begun in this study and summarized in the following paragraphs.

The absorption and stimulated emission cross-section spectra of Er:Sc₂O₃ in the 1558-nm region are shown for several temperatures in figure 9a. Note that although thermal broadening would

normally result in a decrease in peak height as temperature increases (a phenomenon that does affect the 1581-nm peak), the stimulated emission peak cross section remains approximately constant through 150 K. It is this robust stimulated emission cross section at 1558 nm over a temperature range in which the 1581-nm peak weakens that favors 1558-nm laser operation. We interpret this behavior by first noting that there are three transitions in Er:Sc₂O₃ whose spectra overlap at 1558 nm, the three transitions noted in figure 9b. Subsequent to the end of this study, we have integrated over the absorption band in the spectral range of figure 9a for several temperatures and have fit the temperature dependence to a sum of three adjustable line strengths, each multiplied by the thermal population factor applicable to its initial level at each temperature. Obtaining a good fit requires that the second transition (green in figure 9b) be about three times as strong as the lowest transition (red in figure 9b). It is thermal activation of this strong transition that favors lasing at this wavelength well above liquid nitrogen temperature. (The highest-lying of the three transitions appears to make an insignificant contribution to the temperature dependence of the total area. This is due primarily to the much smaller thermal occupation factors involved, but also suggests that its transition strength is not large.)

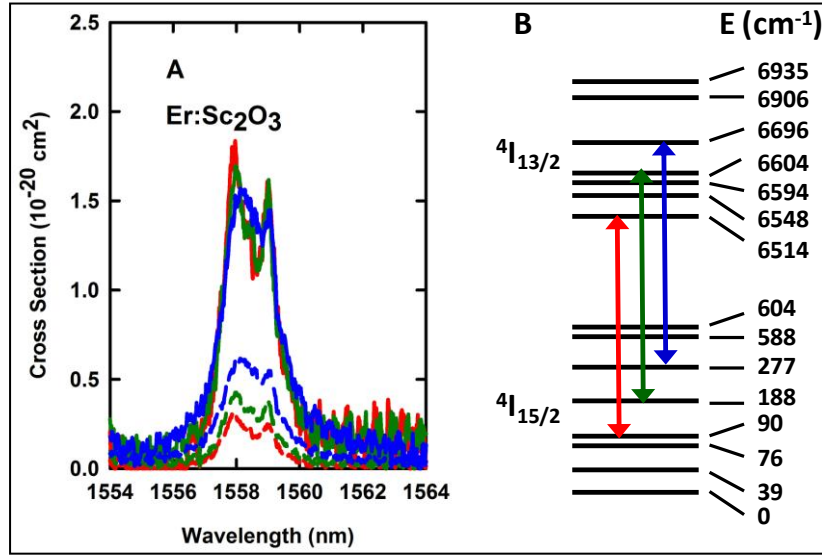


Figure 9. (a) Absorption (dashed curves) and stimulated emission (solid curves) of Er:Sc₂O₃ at three temperatures (red: 77 K; green: 100 K; blue: 150 K); (b) Energy levels of Er:Sc₂O₃, indicating the three overlapping transitions at 1558 nm.

Another feature of Er:Sc₂O₃ makes it favorable for cryogenic laser operation, both at liquid nitrogen temperature and above. That is the observed width of the strong 1535-nm pump line, shown for two low temperatures in figure 10. Of practical interest is the fact that its width is 0.32 nm FWHM at 77 K. This is about a factor of 15 wider than the Er:YAG 1532-nm line at the same temperature, and, of course, it broadens even more as temperature increases. Thus, the use of Er:Sc₂O₃ places far less stringent demands on line narrowing of diode laser pumps. This is the “zero line” (the transition between the lowest-energy levels) of the ⁴I_{13/2} and ⁴I_{15/2}

manifolds, but there is a transition between higher energy levels at almost exactly the same wavelength, and since our best overall energy level scheme puts two additional transitions less than a nanometer away, it is possible that one or both of those is actually close enough to overlap this line. Thus, it is not very surprising that 8-K and 77-K absorption peaks show subtle structure. Fits of this peak to three overlapping lines at both temperatures, performed subsequent to the conclusion of this program, show good agreement with that structure, but require that each component be considerably wider than Er:YAG's very narrow width. Thus, other broadening mechanisms must contribute. Since the ionic size of Er^{3+} is a poor fit for the host Sc^{3+} , 0.089 nm versus 0.0745 nm (5), substantial lattice strain must be expected around each dopant ion. If there is any randomness to this accommodation of the lattice to the dopant, the inhomogeneous broadening may be substantial. This would be a much smaller factor in Er:YAG, as there is a good fit between the sizes of Er^{3+} and Y^{3+} (0.089 nm versus 0.090 nm).

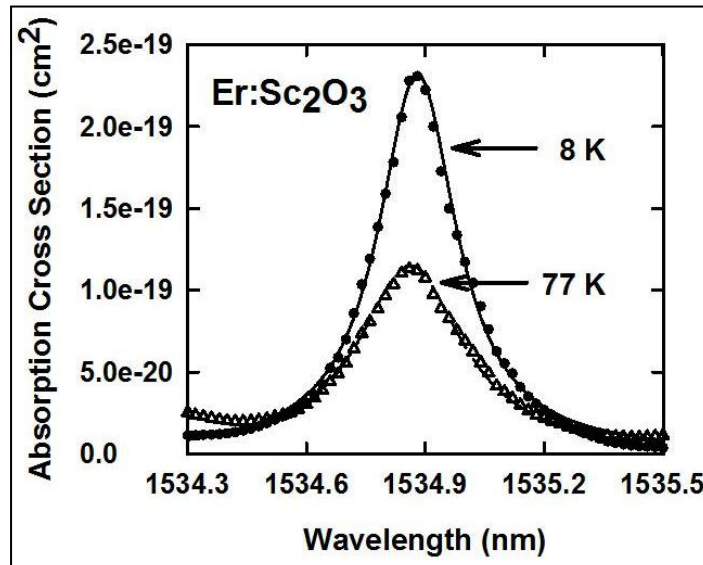


Figure 10. Absorption spectrum of Er:Sc₂O₃ zero-line region at two temperatures.

4. Potential Excited State Absorption in Er:YAG and Er:Sc₂O₃

Up-conversion is complicated, and there was not time to analyze its likelihood in this one-year program. However, it is straightforward to make a preliminary assessment as to whether excited state absorption at the laser wavelength is likely, by comparing the spacings between energy levels with the photon energies of potential laser transitions. Since the energy levels have been refined since the end of this program, the conclusions on potential ESA transitions have also been refined. The results are given in table 2.

Given the typical linewidths of ground state absorption transitions to the upper manifold ($^4I_{9/2}$), only energy level spacings within $\sim 10 \text{ cm}^{-1}$ of the laser photon energy pose a significant risk of ESA at or near 77 K, whereas mismatches of up to $\sim 30 \text{ cm}^{-1}$ conceivably pose such a risk at or near room temperature. From the table, it is evident that there is no risk of ESA at laser wavelengths shorter than about 1600 nm, a particularly favorable result for the operation of Er-doped sesquioxides at wavelengths short enough to minimize the quantum defect. For longer-wavelength lasing at cryogenic temperatures, Er:Y₂O₃ may well face reduced efficiency due to ESA when operating at 1641 nm. The potential problem in Er:Sc₂O₃ is smaller, at least at temperatures near or not far above nitrogen temperature, since the transitions nearly resonant with the 1667-nm laser line initiate at high enough energy to have little thermal population at those temperatures. All three materials have potential ESA issues for long-wavelength lasing at warmer temperatures, where thermal line broadening makes transitions possible with larger energy mismatches. However, it is worth noting that the success of Er:YAG lasers operating at such wavelengths offers evidence that the criteria used in this table may be too conservative (6–9).

Table 2. Potential for excited state absorption at existing or candidate laser wavelengths in the materials under study.

Material	Laser Line (nm)	Transition Matching Within $\sim 10 \text{ cm}^{-1}$ (E's of levels, cm^{-1})	Delta-E (cm^{-1}) ^a	Transition Matching Within $\sim 30 \text{ cm}^{-1}$ (E's of levels, cm^{-1})	Delta-E (cm^{-1}) ^a
Er:YAG	1645	NONE		6599 \rightarrow 12702	50
				6606 \rightarrow 12702	57
	1618	NONE		6549 \rightarrow 12702	0
				6549 \rightarrow 12748	0
				6599 \rightarrow 12748	50
Er:Y ₂ O ₃	1565	NONE		NONE	
	1546	NONE		NONE	
	1641	6510 \rightarrow 12604	0	6510 \rightarrow 12576	0
				6510 \rightarrow 12604	0
				6542 \rightarrow 12604	32
Er:Sc ₂ O ₃	1599	NONE		NONE	
	1579	NONE		NONE	
	1554	NONE		NONE	
	1667	6594 \rightarrow 12593	80	6514 \rightarrow 12520	0
		6604 \rightarrow 12593	90	6548 \rightarrow 12520	34
				6594 \rightarrow 12593	80
				6604 \rightarrow 12593	90
	1605	NONE		NONE	
	1581	NONE		NONE	
	1558	NONE		NONE	

^a Delta-E indicates the distance (in energy) of the initial state of this transition above the bottom of the 4I13/2 manifold. For energy distances smaller than $\sim kT$, the initial state has substantial population, making ESA more likely.

5. Summary and Conclusions

In this program, we began a systematic investigation of laser-related properties of certain Er-doped solids at and above liquid nitrogen temperature, concentrating primarily on Er:YAG and Er:Sc₂O₃. Our goal was to identify and optimize properties that favor operation at temperatures at or above 125–150 K—warm enough to permit cooling by a Stirling cooler, thereby avoiding the need to maintain liquid cryogenics. Although the project did not have time to reach optimized designs and operating schemes, we did identify key features of these materials that favor operation significantly above 77 K.

In Er:YAG, the initial states of the strongest pump line and laser lines lie above the bottoms of their respective Er³⁺ manifolds, so that thermal population is required. This favors higher temperatures, provided one does not go so warm that ground state absorption becomes too large at the laser wavelength. The best pump line in that material is remarkably narrow at 77 K, so

that it would be challenging to line-narrow a diode laser enough to pump it with optimal efficiency. Thus, higher temperatures are favorable due to thermal broadening of this line.

The crystal field splitting of energy levels in Er-doped cubic sesquioxides gives stimulated emission lines at wavelengths considerably closer to the pump line, yet not so close as to give prohibitive absorption at 77–150 K. This permits operation with very small quantum defect, thus making possible the minimization of heating in the gain material. Among the sesquioxides studied, Er:Sc₂O₃ has particularly favorable positioning of energy levels. Its emission line at 1558 nm is not quite as close to the zero line as are similar features in Er:YAG and Er:Y₂O₃, but that is favorable here, as it keeps the 77-K absorption at that line smaller relative to the gain than in those other materials. Its laser operation may represent the smallest quantum defect one can use efficiently at or above liquid nitrogen temperature. Indeed, due to a serendipitous overlap of transitions at that wavelength, with the stronger transition being between higher-energy states, its laser properties remain quite strong up to about 160 K. In work subsequent to this project, we found that this laser line becomes more favorable than a nearby longer-wavelength line as the temperature is increased, opposite the behavior observed in most cryogenic lasers, precisely due to the presence of that strong transition between relatively high-lying levels. Er:Sc₂O₃ has a strong pump line similar in position and strength to that in Er:YAG, but with an order of magnitude greater linewidth. This makes it easier to diode-pump at 77 K and at higher temperatures.

Despite the preliminary status of the laser results achieved in this project, it may be worthwhile to revisit the optimum heat loading estimates made in section 1. In section 3, the best slope efficiency obtained so far was 78% with respect to absorbed pump power (figure 8). Note that this is the pump-lase scheme with a quantum defect of only 1.5%. Although we made a reasonable attempt to match the pump beam size to the anticipated laser mode, we are sure that further optimization of the mode matching is possible. At present, we do not know what fraction of the 20.5% difference between quantum defect limit and observed slope efficiency is due to this imperfect mode matching. By operating the laser far above threshold, the losses due to fluorescence and ground state absorption can be made small. The remaining major unknown is the quantum efficiency of Er:Sc₂O₃. If this is very close to unity, it may be possible to increase the slope efficiency to fairly near the quantum defect limit, but if it is more like 90%, then the slope efficiency would be limited to somewhat below that value. In a different system, (a Ho:YVO₄ slab) our group recently obtained a slope efficiency of 92% with respect to incident pump power at cryogenic temperatures, operating with a quantum defect of 4.9% (10). Thus, if the quantum efficiency of Er:Sc₂O₃ proves to be high, reasonable estimates of the achievable laser efficiency with respect to absorbed pump power (the value relevant in considering the amount of heat deposition) are around 90–95%, with the quantum defect-limited value of 98.5% being a conceivable but unlikely ideal. Given the estimates of Stirling cooler efficiency noted in section 1, this suggests that a more realistic energy budget for removing the heat from the gain

medium is 20–50% of the laser output, rather than the ideal 8–12% estimated there. As also noted in section 1, the amount of power wasted as heat in the pump diodes is roughly equal to the laser output power in an efficient system. Thus, the practicality of a liquid-nitrogen-free cryogenic laser will depend rather sensitively on where the actual performance falls within this estimated range. An energy budget near the lower end, ~20–25% of the laser’s output power, and thus ~10-13% of the total electrical power, may be worthwhile to eliminate cryogenic liquids from the laser system’s logistics train.

Knowing the features of Er:YAG and Er:Sc₂O₃ that favor good performance at temperatures above that of liquid nitrogen, it should be possible to design laser operating schemes—Er concentration, gain medium length, pump wavelength, and cavity optics—to optimize performance in the desired 125–150 K range. Due to the brevity of this project, we did not get far enough to tell whether the advantages noted here would be enough to overcome the increased laser threshold that must be expected due to higher absorption at higher temperatures. However, the properties and laser results observed in this project are promising.

6. References

1. Ter-Gabrielyan, N.; Dubinskii, M.; Newburgh, G. A.; Michael, A.; Merkle, L. D. Temperature Dependence of a Diode-Pumped Cryogenic Er:YAG Laser. *Opt. Expr.* **2009**, *17* (9), 7159–7169.
2. Aggarwal, R. L.; Ripin, D. J.; Ochoa, J. R.; Fan, T. Y. Measurement of Thermo-Optic Properties of $\text{Y}_3\text{Al}_5\text{O}_{12}$, YAlO_3 , LiYF_4 , LiLuF_4 , BaY_2F_8 , $\text{KGd}(\text{WO}_4)_2$, and $\text{KY}(\text{WO}_4)_2$ Laser Crystals in the 80–300 K Temperature Range. *J. Appl. Phys.* **2005**, *98*, 103514.
3. Klein, P. H.; Croft, W. J. Thermal Conductivity, Diffusivity, and Expansion of Y_2O_3 , $\text{Y}_3\text{Al}_5\text{O}_{12}$, and LaF_3 in the Range 77°–300°K. *J. Appl. Phys.* **1967**, *38* (4), 1603–1607.
4. Mun, J. H.; Jouini, A.; Novoselov, A.; Yoshikawa, A.; Kasamoto, T.; Ohta, H.; Shibata, H.; Isshiki, M.; Waseda, Y.; Boulon G.; Fukuda, T. Thermal and Optical Properties of Yb^{3+} -Doped Y_2O_3 Single Crystal Grown by the Micro-Pulling-Down Method. *Jap. J. Appl. Phys.* **2006**, *45* (7), 5885–5888.
5. Shannon, R. D. Revised Effective Ionic Radii and Systematic Studies of Interatomic Distances in Halides and Chalcogenides. *Acta Cryst. A* **1976**, *A32*, 751–767.
6. Garbuzov, D.; Kudryashov, I.; Dubinskii, M. Resonantly Diode Laser Pumped 1.6- μm -Erbium-Doped Yttrium Aluminum Garnet Solid-State Laser. *Appl. Phys. Lett.* **2005**, *86*, 131115.
7. Garbuzov, D.; Kudryashov, I.; Dubinskii, D. M. 110 W(0.9 J) Pulsed Power from Resonantly Diode-Laser-Pumped 1.6- μm Er:YAG Laser. *Appl. Phys. Lett.* **2005**, *87*, 121101.
8. Setzler, S. D.; Francis, M. P.; Young, Y. E.; Konves, J. R.; Chicklis, E. P. Resonantly Pumped Eyesafe Erbium Lasers. *IEEE J. Sel. Top. in Quantum Electronics* **2005**, *11* (3), 645–657.
9. Setzler, S. D.; Francis, M. W.; Chicklis, E. P. A 100 mJ Q-switched 1645 nm Er:YAG Laser. *SPIE Defense and Security Symposium* **2007**, paper 6552–17.
10. Newburgh, G. A.; Fleischman, Z.; Dubinskii, M. Highly Efficient Dual-Wavelength Laser Operation of Cryo-Cooled Resonantly (in-band) Pumped Ho^{3+} :YVO₄ Laser. *Opt. Lett.* **2012**, *37* (18), 3888–3890.

1 (PDF)	DEFENSE TECH INFO CTR ATTN DTIC OCA (PDF)
1 (PDF)	GOVT PRNTG OFC ATTN A MALHOTRA
1 (PDF)	HEL-JTO ATTN W FINK
9 (PDFS)	US ARMY RSRCH LAB ATTN RDRL SEE M G NEWBURGH ATTN RDRL SEE M J ZHANG ATTN RDRL SEE M L MERKLE ATTN RDRL SEE M M DUBINSKIY ATTN RDRL SEE M N TER-GABRIELIAN ATTN RDRL SEE M T SANAMYAN ATTN RDRL SEE M Z FLEISCHMAN ATTN IMAL HRA MAIL & RECORDS MGMT ATTN RDRL CIO LL TECHL LIB